Rheologica Acta Rheol Acta 25:55–61 (1986)

Influence of disperse phase concentration upon the viscoelastic behaviour of emulsions

N. Gladwell, R. R. Rahalkar, and P. Richmond

AFRC Food Research Institute, Norwich (England)

Abstract: Rheology of soya oil-water emulsions in the linear region has been studied. The viscoelastic response consisted of three contributions. There was a purely elastic component, a purely viscous component and a contribution due to the retarded compliance. Emulsions became more viscous and elastic with increasing soya oil concentration. Sharp changes in rheology were observed as the concentration approached the random close packed limit. There was also a marked increase in zero-shear viscosity. Breakdown of coagulation structure was observed as the shear stress was increased into the non-linear region. The rheological behaviour of the emulsions in the linear region could be adequately described by the generalized Kelvin-Voigt model.

Key words: Soya oil-water emulsion, creep-recovery behaviour, retardation-time spectrum, linear rheological behaviour, nonlinear rheological behaviour, coagulation structure

1. Introduction

Knowledge of the rheological behaviour of emulsions is useful in understanding the interaction forces between the emulsion droplets. In oil-water emulsions, three-dimensional network-like structures can be formed due to colloidal interactions between the oil droplets. The network structure is capable of storing energy, giving rise to an elastic solid-like behaviour (usually in addition to the liquid-like behaviour).

The viscoelastic properties of liquids and emulsions are generally studied at low deformations so as to minimize the possibility of structure breakdown. It is possible to obtain information regarding thixotropy or shear thinning behaviour using high deformations. However, it is usually difficult to correlate these data with the structure at low deformations or at rest. When the system is perturbed from the equilibrium state, the resulting response can be divided into two parts. In response to the applied stress, there is an instantaneous increase in strain, followed by a slow increase with time to the equilibrium value. When the stress is released, there is an instantaneous component to the strain recovery, which is followed by the time-dependent recovery. The entire response constitutes the creep recovery behaviour.

The creep recovery experiments may be carried out under constant stress or constant strain. If a constant shear stress σ is applied at time zero, the creep compliance at time t is given by

$$J(t) = \gamma(t)/\sigma\,, \tag{1}$$

where $\gamma(t)$ is the strain at time t. For a viscoelastic fluid, the creep response is given by,

$$J(t) = J_0 + J_e\,\psi(t) + t/\eta\,, \tag{2}$$

where J_0, J_e and η are the instantaneous compliance, retarded compliance and zero shear viscosity respectively. The retardation function $\psi(t)$ is given by

$$\psi(t) = \frac{1}{J_e}\int_{-\infty}^{\infty} L(\tau)\,[1-\exp(-t/\tau)]\,d\ln\tau\,. \tag{3}$$

$L(\tau)$, the retardation time spectrum may be approximated by the Schwarzl method [1]:

$$L(\tau) = \frac{d}{d\ln\tau}\,[J(t) - t/\eta]\,. \tag{4}$$

If the retardation time spectrum is known, the relationship between $J(t)$ and t may be obtained. Alternatively, a series of discrete retardation times (instead of a continuous spectrum) may be assumed:

$$J(t) = J_0 + \sum_i J_i[1-\exp(-t/\tau_i)] + t/\eta\,. \tag{5}$$

J_i is the retarded compliance of the i-th component with retardation time τ_i. Eqs. (2) and (5) represent the generalized Kelvin-Voigt model [2, 3].

In the linear region, the parameters J_0, J_i, τ_i and η are independent of the applied stress, while they vary with the stress in the nonlinear region due to the breakdown of structure. It is possible to describe the recovery behaviour using the same set of parameters. Creep recovery measurements over a period of time sufficiently greater than the longest retardation time thus present an opportunity to study the viscous and elastic components separately.

In the literature, the viscoelastic behaviour of emulsions and suspensions has been reported by several authors. Similar creep recovery behaviour has been observed for the emulsions of Nujol in water and water in Nujol [4, 5], paraffin oil in water [6], and for suspensions of polystyrene latex in water [7, 8], TiO_2 in water [7], carbon black in oil [9] and bentonite in water [10, 11]. Evidently, the rheology of coagulation structure is similar for many emulsions and dispersions. In this paper, we report the rheology of food emulsions with a view to understanding the coagulation structure and its dependence upon the disperse phase volume fraction (φ). Both water/oil and oil/water emulsions are quite common in the food industry. An understanding of the rheology and microstructure of the emulsions is necessary for analysing and eventually improving the processing performance of food products such as mayonnaise, salad creams, butter and margarine.

2. Materials and experimental methods

Deionized water was used for the preparation of emulsions. Deionization was carried out in two stages. The first stage was a TSA 300 twin bed with weak base anion resin. The second stage was a MB12 mixed bed. Both the twin bed and the mixed bed were supplied by Permutit Services Ltd. Commercially available soyabean oil supplied by Petty, Wood & Co was used. Dried egg yolk powder was supplied by Colman's of Norwich. Xanthum gum was ex KELCO/AIL and was supplied by Colman's of Norwich.

Fatty acid composition of soya oil was determined by gas chromatography of the derived methyl esters. 100 mg of the oil were converted to methyl esters of the fatty acids by reactions with 1 ml of 0.05 M sodium methoxide in methanol for 30 minutes at 60 °C. After cooling, 20 ml of dilute aqueous sulfuric acid (0.01 M) were added and the precipitated esters extracted with hexane. The hexane extracts were dried, filtered and the solvent removed by rotary evaporation. The esters were then dissolved in 2,2,4 trimethyl pentane for gas chromatography.

A Carlo Erba MEGA 5160 gas chromatograph fitted with a flame ionisation detector was used. 0.5–1 µl of methyl ester solution was injected into a column (2 m × 3 mm i.d.) packed with 3% SP–2310/2% SP–2300 on 100–120 mesh chromosorb W-AW (Supelco Inc; U.S.A.). The column oven was maintained at 200 °C. Methyl esters were identified by comparison with a mixture of known composition and percentage compositions were calculated from peak areas using a computing integrator.

2.1 Preparation of emulsions

Six emulsions were prepared, with the volume fraction of oil (φ) of 0.2, 0.3, 0.4, 0.5, 0.6 and 0.7. The proportion of xanthan to water was kept constant throughout at 0.018. Egg yolk was used as an emulsifier. The volume fraction of egg yolk was kept constant at 0.03 for all the emulsions. The emulsions were prepared using a commercial Waring food blender and the typical shearing time was 2–3 minutes.

2.2 Droplet size measurements

Size distribution measurements were carried out using a Malvern particle size analyser model 2600 HSD. A description of the instrument is given elsewhere [12]. As with other sizing techniques, it was necessary to dilute the emulsions, the volume fraction of oil in the diluted emulsions being less than 0.001 in all cases. The emulsions were diluted in deionized distilled water and no dispersing agent was necessary for dilution.

2.3 Density

Density of soya oil was measured on a Paar DMA 602 density meter. Approximately 1 ml of oil was introduced in a *U* tube sample cell. The measuring principle is based on the change of natural frequency of a hollow oscillator filled with the sample. There exists a simple relationship between the density of the sample and the natural frequency of resonance of a filled oscillator.

2.4 Surface tension

Interfacial tension between soya oil and water was measured by a standard pendant drop technique. A syringe was filled with water and a drop was formed at the tip of the syringe needle in the surrounding medium of soya oil. The dimensions of the drop were measured by a travelling microscope. The interfacial tension was calculated from the dimensions of the drop and the densities of the two liquids.

2.5 Viscosity

At low and moderate shear rates, soya oil behaves like a Newtonian liquid. The viscosity was measured by a standard *U* tube Cannon-Ubbelohde Viscometer and also by a Contraves Rheomat 115 (shear rate 5 s^{-1} to 1000 s^{-1}).

2.6 Rheology

The creep recovery measurements were carried out using a series II Deer rheometer. In order to study the emulsion structure, it was necessary to apply very low deformations. A concentric cylinder assembly was used for this purpose, the diameters of inner and outer cylinder being 12 mm and 15 mm respectively. The outer cylinder was held stationery, while the inner one could be subjected to a fixed torque, thereby apply-

ing constant stress. The strain increases in response to the applied stress. The stress is then removed and the strain relaxation is observed, the two responses together giving the creep-recovery behaviour. The shear stress ranged from 0.5 to 10 Pa, while the shear rate ranged from $2 \cdot 10^{-5}$ to $6 \cdot 10^{-4} s^{-1}$. Calculations of shear stress, shear strain and the end effect corrections were made by standard procedures [13].

The measurements were carried out at several stress values for each emulsion in the linear region and the data for each emulsion was averaged over at least four shear stresses. In addition, all the emulsions were prepared several times and the average was taken. The reproducibility between independent measurements of different emulsions with the same composition was better than 90%, of all the steps the emulsion preparation being the least reproducible. Density, viscosity, surface tension and rheological measurements were carried out at 22 ± 0.1 °C.

3. Results and discussion

Table 1 summarizes the properties of soya oil. The emulsions were characterized by measuring the droplet size distributions. Using the Malvern particle size analyser, the size distribution was obtained as the weight percentage of droplets in several different size bands. Three typical size distributions are shown in figure 1. The size distributions for the other emulsions were comparable and the average droplet diameter varied between 3.1 μm and 3.4 μm. The lower limit for the measurements was 1.2 μm. In each emulsion, approximately 10% of the droplets were smaller than 1.2 μm.

Figure 2 shows the variation of strain with time for $\varphi = 0.6$ emulsion for different values of stress. All the curves reduce to a single $J(t)$ vs. time curve in the linear region. Similar curves were obtained for other emulsions. Figure 3 shows the compliance behaviour of the emulsions. In the case of all emulsions, three separate processes can be identified. The first process is an instantaneous one, where the compliance increases from zero to J_0 instantaneously or over a very short period of time. The second process is slower, where the compliance slowly creeps to the equilibrium

Table 1. Physico-chemical properties of soyabean oil

Fatty acid composition:	
Palmitic acid	9.8%
Stearic acid	3.9%
Oleic acid	20.1%
Linoleic acid	57.0%
Linolenic acid	7.1%
Density	919.8 kg/m^3
Viscosity	0.0804 Pa · s
Soya oil/water interfacial tension	19 mN/m

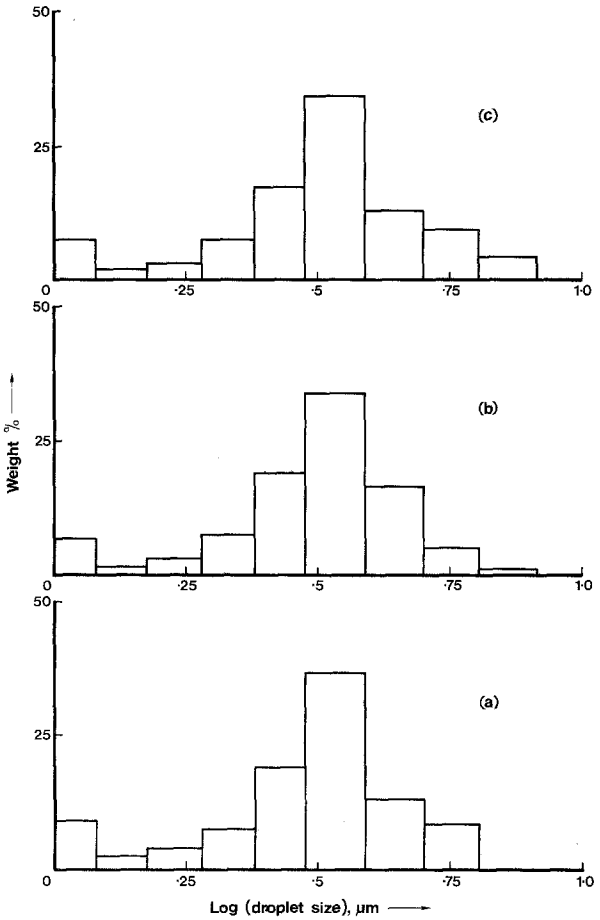

Fig. 1. Particle size distributions of oil/water emulsions with φ = (a) 0.2, (b) 0.4 and (c) 0.6

value. Superimposed upon this process is the viscous flow. The flow was observed in all the emulsions, the contribution to the creep compliance being given by t/η. Thus these emulsions do not behave as rigid gels, but as viscoelastic liquids. The viscoelastic response could be adequately described by assuming two retardation processes. Substituting $i = 2$ in eq. (5),

$$J(t) = J_0 + J_1 \exp(-t/\tau_1) + J_2 \exp(-t/\tau_2) + t/\eta . \quad (6)$$

It was possible to obtain good fit with the experimental data by using eq. (6). This model is compared with the data in figure 4. The points are experimental values, while eq. (6) is represented by the continuous curves. Similar models with two retardation processes have been reported by Maron and Sisko [8] and by Sherman [4].

The variation of rheological parameters with φ is shown in figure 5 (J_0, J_1, J_2) and figure 6 ($\eta, \eta_1 = \tau_1/J_1, \eta_2 = \tau_2/J_2$). The values of these parameters are listed in table 2. The emulsions become more elastic as

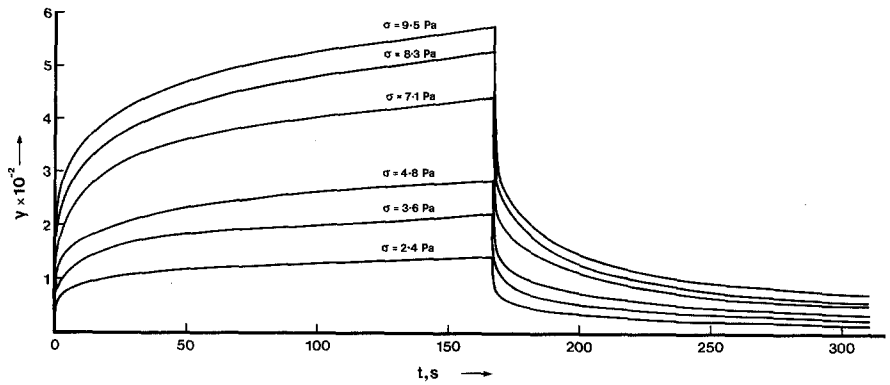

Fig. 2. Variation of strain with time for $\varphi = 0.6$ emulsion. Shear stress (σ) values as indicated

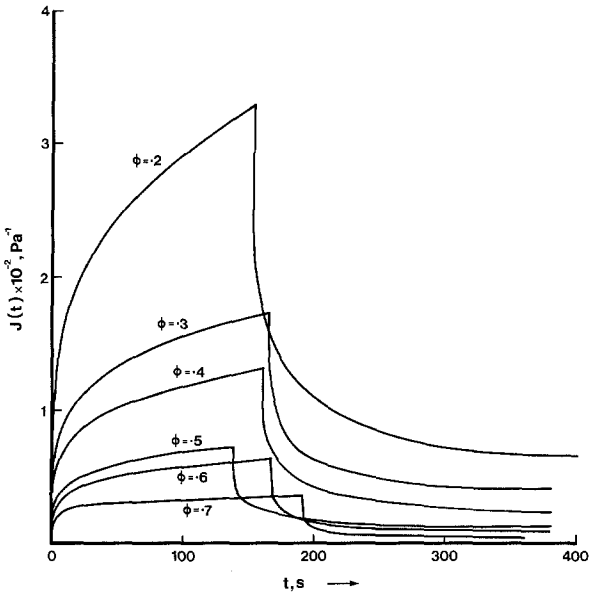

Fig. 3. Creep recovery response of soya oil-water emulsions. Oil phase concentration as indicated

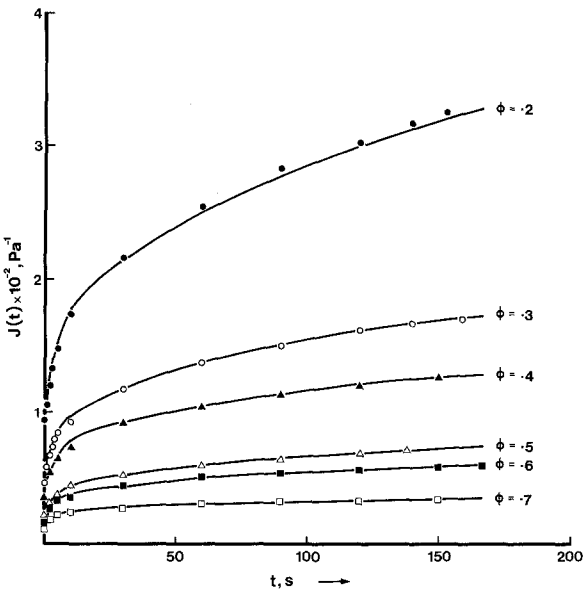

Fig. 4. Curve fitting of experimental creep compliance data to the two retardation process Kelvin-Voigt model. φ values as indicated

Table 2. Linear viscoelastic parameters for soya oil-water emulsions

Disperse phase (soya oil) concentration %	J_0 Pa^{-1}	J_1 Pa^{-1}	J_2 Pa^{-1}	η Pa·s	η_1 Pa·s	η_2 Pa·s
20	$7.9 \cdot 10^{-3}$	$1.3 \cdot 10^{-2}$	$6.7 \cdot 10^{-3}$	$2.4 \cdot 10^{4}$	$6.3 \cdot 10^{3}$	$5.1 \cdot 10^{2}$
30	$4.6 \cdot 10^{-3}$	$7.8 \cdot 10^{-3}$	$4.0 \cdot 10^{-3}$	$5.6 \cdot 10^{4}$	$1.0 \cdot 10^{4}$	$5.5 \cdot 10^{2}$
40	$3.6 \cdot 10^{-3}$	$4.3 \cdot 10^{-3}$	$3.9 \cdot 10^{-3}$	$7.6 \cdot 10^{4}$	$2.1 \cdot 10^{4}$	$9.8 \cdot 10^{2}$
50	$2.1 \cdot 10^{-3}$	$2.8 \cdot 10^{-3}$	$2.0 \cdot 10^{-3}$	$1.4 \cdot 10^{5}$	$2.3 \cdot 10^{4}$	$1.5 \cdot 10^{3}$
60	$1.7 \cdot 10^{-3}$	$1.9 \cdot 10^{-3}$	$1.9 \cdot 10^{-3}$	$1.9 \cdot 10^{5}$	$3.3 \cdot 10^{4}$	$1.6 \cdot 10^{3}$
70	$1.2 \cdot 10^{-3}$	$1.2 \cdot 10^{-3}$	$1.1 \cdot 10^{-3}$	$4.9 \cdot 10^{5}$	$4.3 \cdot 10^{4}$	$2.1 \cdot 10^{3}$

J_0 – instantaneous elastic compliance, J_1, J_2 – retarded elastic compliances, η – zero shear-rate viscosity, η_1, η_2 – retarded viscosities

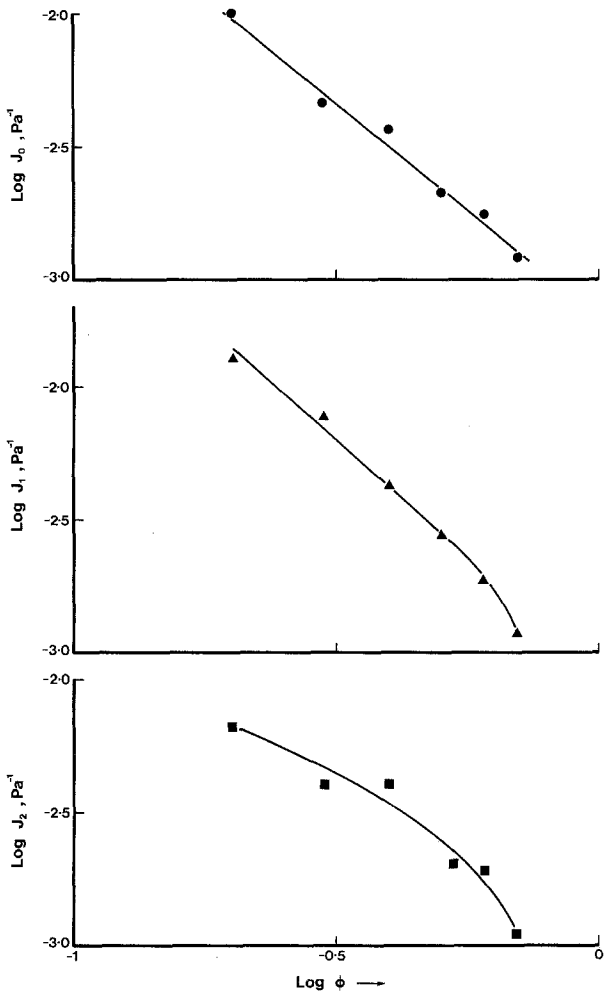

Fig. 5. Variation of the instantaneous compliance J_0 and the retard compliances J_1 and J_2 with φ in the linear region

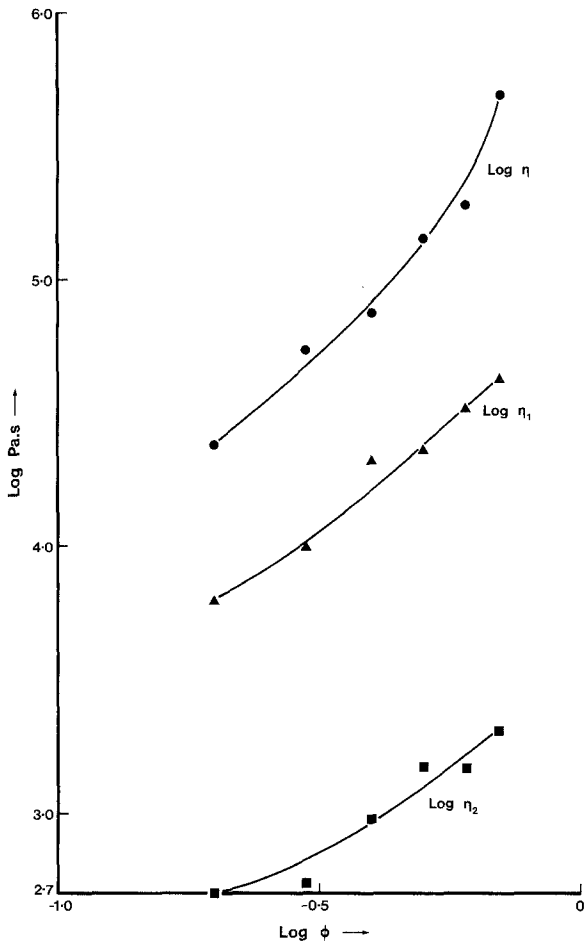

Fig. 6. Variation of the zero shear-rate viscosity η and the retarded viscosities η_1 and η_2 with φ in the linear region (viscosities in Pa · s)

φ is increased, which is reflected in the decrease in the compliance values and increase in the retarded viscosities η_1 and η_2. The zero-shear-rate viscosity η also increases with oil content. However, at higher concentrations, the rate of increase of η, η_1 and η_2 also increases. Similarly, while J_1 follows the power-law dependence over most of the concentration range, there is a sharp drop in J_1 values for $\varphi = 0.6$ and $\varphi = 0.7$ emulsions. Similar marked changes in emulsion rheology with increasing φ have been reported previously [12]. If the droplets are assumed to be rigid non deformable spheres, there is an upper limit of 0.64 for the random close packing of uniform spheres in three dimensions [14]. For a polydisperse emulsion, this figure would be greater, since the smaller droplets can be packed into the void spaces formed by the packing of larger droplets. The $\varphi = 0.7$ emulsion is in this dense close packed region and a considerable amount of interdroplet interactions are expected. Since φ is greater than the random close packed fraction, the droplets are probably deformed and some of the increase in elasticity may be attributed to the distortion of oil droplets. Molecules of egg yolk lipoproteins, which act as emulsifier, are adsorbed at the oil-water interface. When the droplets are close together or almost touching each other there will be strong protein-protein and protein-polysaccharide interactions. Van der Waals interactions also play a significant role in governing the rheology of emulsions [15, 16]. These interactions are probably responsible for the enhanced elasticity of the more concentrated emulsions.

The two retardation times in eq. (6) represent the average of the retardation processes involved. More detailed information about the distribution of retardation times can be obtained from eq. (4) by taking the slope of the plot of $J(t) - t/\eta$ vs. $\ln(t)$ at various values of t. Figure 7 shows the variation of $L(\tau)$ with t for the emulsions. The retardation spectra are similar to those

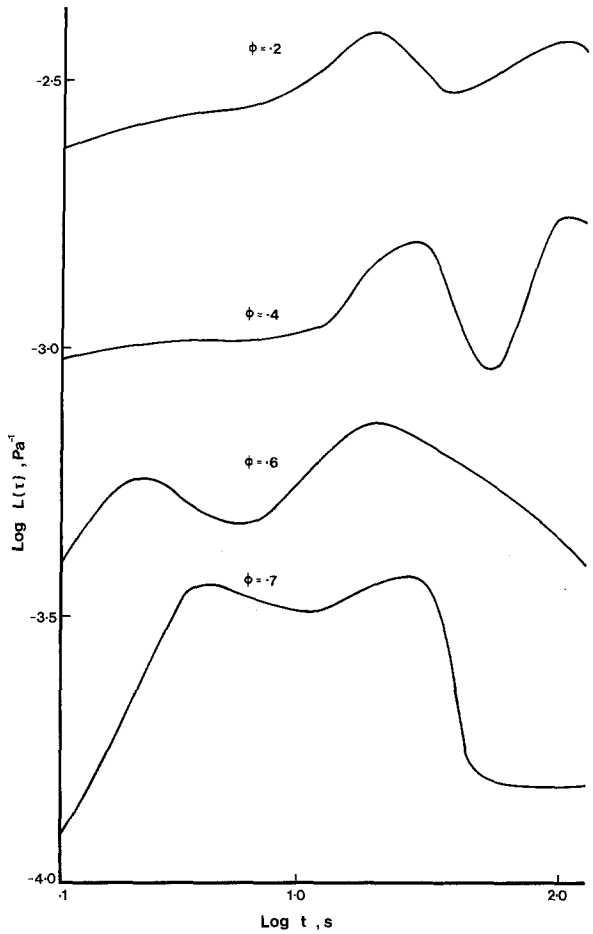

Fig. 7. Retardation-time distribution spectra for the emulsions. φ values as indicated

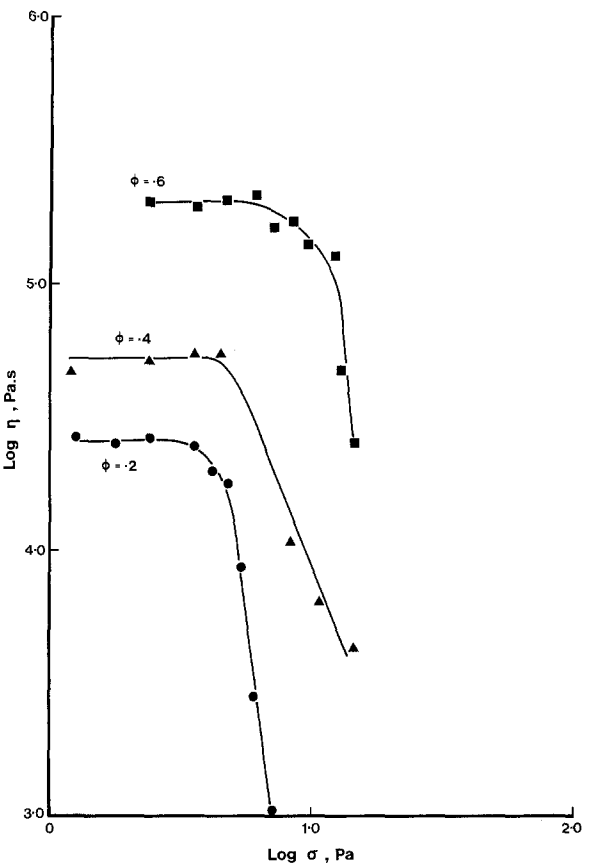

Fig. 9. Breakdown of coagulation structure in the non-linear region. Plot of zero-shear viscosity vs. shear stress. φ values as indicated

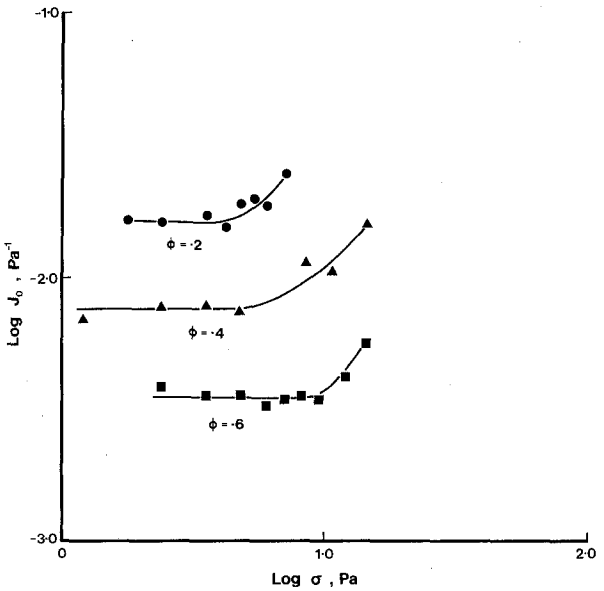

Fig. 8. Breakdown of coagulation structure in the non-linear region. Plot of instantaneous compliance vs. shear stress. φ values as indicated

obtained by Sherman for 50% water/Nujol emulsions [4] but different from those for 62.5% water/Nujol emulsions [5]. At least two retardation mechanisms can be identified. As φ is decreased, the faster of the two mechanisms disappears while the slower process ($t \cong 22$ s) becomes more pronounced. A still slower mechanism around $t \cong 100$ s, contributes at lower values of φ. The dominance of the slower mechanisms indicates that the dilute emulsions are less elastic. According to Sherman, one of the retardation processes is due to the droplets smaller than 0.5 μm. All our emulsions contained comparable amounts of droplets smaller than 1.2 μm. Hence, one of the mechanisms could possibly be attributed to the presence of smaller droplets. The emulsifier and xanthan molecules are adsorbed on the surface of the droplets. The interactions between these molecules are likely to be much stronger when the droplets are closer together (in concentrated emulsions). The presence of similar interactions (polyelectrolyte bridging) has been postulated

by Lyklema et al. [6]. One of the retardation mechanisms may be due to these interactions. In relatively dilute emulsions ($\varphi = 0.2, 0.4$) the number of interactions per unit volume would be smaller and the retardation slower. The retardation mechanism would then operate on a longer time scale.

The creep/recovery behaviour is independent of the applied stress in the linear region. In the non-linear region, breakdown of the coagulation structure occurs in response to the applied stress, resulting in an increase in J_0 and a decrease in viscosity. To monitor the structure breakdown, J_0 and η are plotted against the applied stress in figures 8 and 9 respectively. The breakdown is very rapid in the non-linear region, as seen from the viscosity values. Viscous contribution to the total compliance t/η becomes dominant in the non-linear region as t increases and η decreases. Instantaneous compliance J_0 increases with the applied stress, but to a much smaller extent. The linear range for J_0 is greater than the linear range for viscosity. Similar 'loss of coherence' in the upper end of the linear region has been reported in the literature [6].

Food emulsions in general are complex systems, and much theoretical work still needs to be done to get a better understanding of colloidal interactions and their effect upon rheology and microstructure. However, the rheological measurements upon various systems as reported in the literature form a basic pattern and our study indicates that food emulsions may well form a part of that pattern.

Acknowledgement

The authors are grateful to Dr. A. M. Howe for measuring the oil-water interfacial tension and to Mr. K. E. Peers for measuring the fatty acid composition of soya oil.

References

1. Leaderman H (1958) In: Eirich FR (ed), Rheology, theory and applications, vol 2. Academic Press, New York
2. Bland DR (1960) The theory of linear viscoelasticity. Pergamon Press, New York
3. Purkaystha S, Peleg M, Normand MD (1984) Rheol Acta 23:556
4. Sherman P (1967) J Colloid Interface Sci 24:107
5. Sherman P (1970) In: Onogy S (ed) Proc V. Intern Congr Rheol vol 2, p 327. University of Tokyo Press
6. Lyklema J, van den Tempel M, van Vliet T (1978) Rheol Acta 17:525
7. Zosel A (1982) Rheol Acta 21:72
8. Maron SH, Sisko AH (1957) J Colloid Sci 12:99
9. Payne AR (1964) J Colloid Sci 19:744
10. Rehbinder P (1965) Pure Appl Chem 10:337
11. Rehbinder P (1970) In: Onogy S (ed) Proc V. Intern Congr Rheol, vol 2, p 375. University of Tokyo Press
12. Hennock M, Rahalkar RR, Richmond P (1984) J Food Sci 49:1271
13. Whorlow RW (1980) Rheological Techniques. J. Wiley, London
14. Scott GD (1960) Nature 108:908
15. Verwey EJW, Overbeek ITG (1948) Theory of the stability of lyphobic colloids. Amsterdam
16. Derjaguin BV, London LD (1941) Acta Phys Chim USSR 14:633

(Received February 14, 1985;
in revised form March 25, 1985)

Authors' address:

Mr. N. Gladwell, Dr. R. R. Rahalkar*), Dr. P. Richmond
AFRC Food Research Institute
Colney Lane
Norwich NR4 7UA (England)

*) To whom communications should be addressed.